PROCEEDINGS OF SCIENCE

Performance of Monte Carlo Event Generators for the Production of Boson and Multi-Boson States ATLAS Analysis

Francesco Giuli[*†]
University of Oxford
E-mail: francesco.giuli@cern.ch, francesco.giuli@physics.ox.ac.uk

The Monte Carlo (MC) setups used by ATLAS to model boson+jets and multi-boson processes at $\sqrt{s} = 13$ TeV in proton-proton collisions are described. Comparisons between data and several event generators are provided for key kinematic distributions. Issues associated with the evaluation of systematic uncertainties are also discussed. This proceeding is a summary of the results collected in two recent ATLAS PUB notes published for the MC workshop jointly-organised by the the ATLAS and CMS Collaborations and held at CERN in May 2017.

EPS-HEP 2017, European Physical Society conference on High Energy Physics
5-12 July 2017
Venice, Italy

[*]Speaker.
[†]on behalf of the ATLAS Collaboration

PoS(EPS-HEP2017)737

Introduction This proceeding describes the Monte Carlo (MC) used by ATLAS [1] to model boson+jets (V + jets) [2] and multi-boson (VV/VVV) [3] processes in 13 TeV pp collisions. The baseline MC generators are compared with each other in key kinematic distributions of the processes under study. Sample normalisation and assignment of systematic uncertainties are discussed.

Boson+jets The setup of the samples used for the different comparisons is described in the following:

- **Sherpa** `Sherpa` [4] is a parton shower MC generator simulating additional hard parton emissions that are matched to a parton shower based on Catani-Seymour subtraction terms [5]. The merging of multi-parton matrix elements (ME) with the parton shower (PS) is achieved using an improved CKKW matching procedure [6, 7], which is extended to next-to-leading order (NLO) accuracy using the MEPS@NLO prescription [8].

- **MadGraph5_aMC@NLO using CKKW-L** Matrix elements for V+ up to 4 partons at LO accuracy are produced using `MadGraph5_aMC@NLO v2.2.2` [9] interfaced with `Pythia v8.186` [10] for the modelling of the parton shower and underlying event. The CKKW-L matching [6, 11] and merging procedure is applied, with a merging scale (μ_Q) of 30 GeV. The NNPDF3.0NLO PDF set is used with $\alpha_s = 0.118$ and the A14 tune of Pythia8 [12] is applied.

- **MadGraph5_aMC@NLO using FxFx** Samples have also been generated using the `MadGraph5_aMC@NLO` program to generate matrix elements for V + 0, 1 and 2 partons to NLO accuracy. The showering and subsequent hadronisation has been performed using Pythia 8.210 with the A14 tune, using the NNPDF2.3LO PDF set with $\alpha_s = 0.13$. The different jet multiplicities are merged using the FxFx prescription [13] implemented in the `MadGraph5_aMC@NLO` program (version 2.3.3 is used here). The impact of various μ_Q has been studied, analysing three different values: 20 GeV (downward variation), 25 GeV (nominal value) and 50 GeV (upward variation).

- **Powheg MINLO** Predictions from `Powheg MiNLO` [14, 15, 16] interfaced to Pythia 8.210 [10] with the AZNLO tune [17] were obtained to produce V + jets events. The PDF set used in Powheg is CT14NNLO [18] whereas the PDF set used in the parton shower is the CTEQ6L1 [19] LO set.

Figure 1 shows comparisons of `Sherpa 2.2` (red), `Powheg MiNLO+Py8` (blue) and `MG5_aMC@NLO+Py8` using FxFx (green) against data (black) from the 13 TeV ATLAS Z + jets measurement [20]. The measurement uncertainty is indicated by a grey band in the ratio panels, while generator uncertainties have been estimated using Sherpa 2.2 and are indicated by the orange band in the ratio panels. The MEPS@NLO setup using Sherpa 2.2 is NLO-accurate for up to two extra emissions and LO-accurate for up to four extra emissions. At very high jet multiplicities, Sherpa 2.2 starts to diverge from the data, indicating too much activity in the PS. The `MG5_aMC@NLO` setup already begins to mismodel the data for lower multiplicities, as it lacks additional multilegs beyond the third emission, making it less attractive for many new-physics searches interested in a good modelling of high multijet configurations, even though the mismodelling is likely covered by

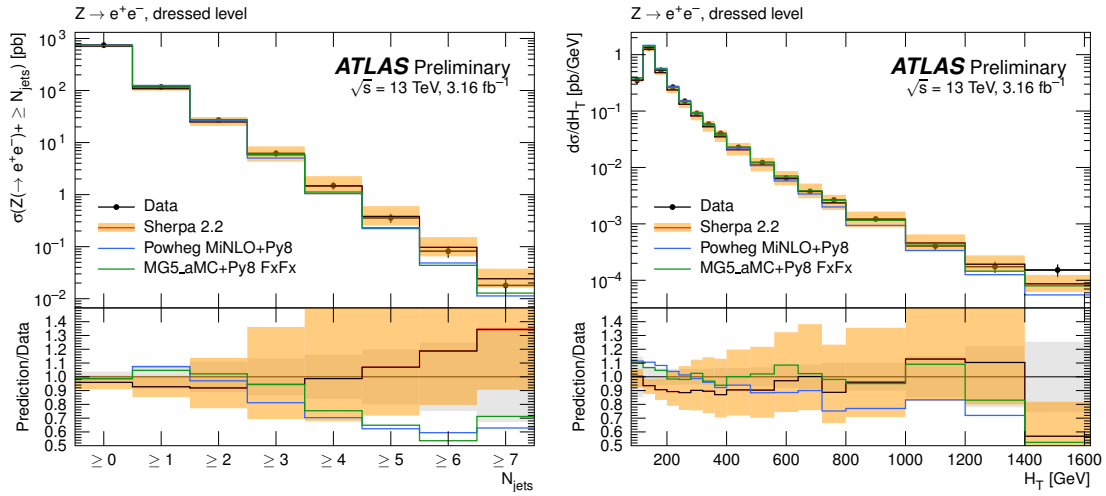

(a) (b)

Figure 1: Predictions for the differential cross sections as a function of the inclusive jet multiplicity (left) and of the scalar jet-p_{T} sum, H_{T}, (right) from `Sherpa 2.2` (red), `Powheg MiNLO+Pythia8` (blue) and `MG5_aMC@NLO+Py8` using FxFx (green). The predictions are compared to data (black) from a recent ATLAS measurement of $Z+$jets production [20]. These plots are taken from Ref. [2].

the scale uncertainties. A similar comparison for the first- and third-order splitting scale distribution occuring in the k_t algorithm [21, 22] is shown in Figure 2 between `Sherpa 2.2` (red) and `MG5_aMC@NLO+Py8` using FxFx (blue) at a centre-of-mass energy of 13 TeV. Generator uncertainties have been estimated using `Sherpa 2.2` and are indicated by the orange band in the ratio panels. In addition, variations of the FxFx matching scale, μ_Q, (shown in solid and dashed green) have been studied for the `MG5_aMC@NLO+Py8` setup. The statistical uncertainty component is indicated by the error bars. It can be seen that neither the PDF and scale variations estimated using `Sherpa 2.2` nor the matching-scale variations estimated for the FxFx setup can cover the differences between the two predictions seen in the transition region, e.g. $\sqrt{d_k} \approx 5$ GeV, between the soft and the perturbative regimes, where $\sqrt{d_k}$ is the associated splitting scale defined in Ref. [23].

Multi-boson

Fully leptonic diboson processes The processes can be grouped according to the number of charged leptons, giving rise to the following final states: 4ℓ, $3\ell\nu$, $2\ell 2\nu$, $\ell 3\nu$ and 4ν. An overview of the accuracy achieved with the chosen generators is given in Table 1. A general shape comparison between `PowhegBox` and `Sherpa v2.2` is shown in Figure 3(a).

The distributions are normalised to the samples' cross section and there is no reweighting applied.

	$VV+0j$	$VV+1j$	$VV+2j$	$VV+3j$	$VV+\geq 4j$
`Sherpa v2.2`	NLO	NLO	LO	LO	PS
`PowhegBox+PYTHIA8/Herwig++`	NLO	LO	PS	PS	PS
`MadGraph5_aMC@NLO+PYTHIA8`	NLO	NLO	LO	PS	PS

Table 1: Overview of process accuracies for the chosen generators.

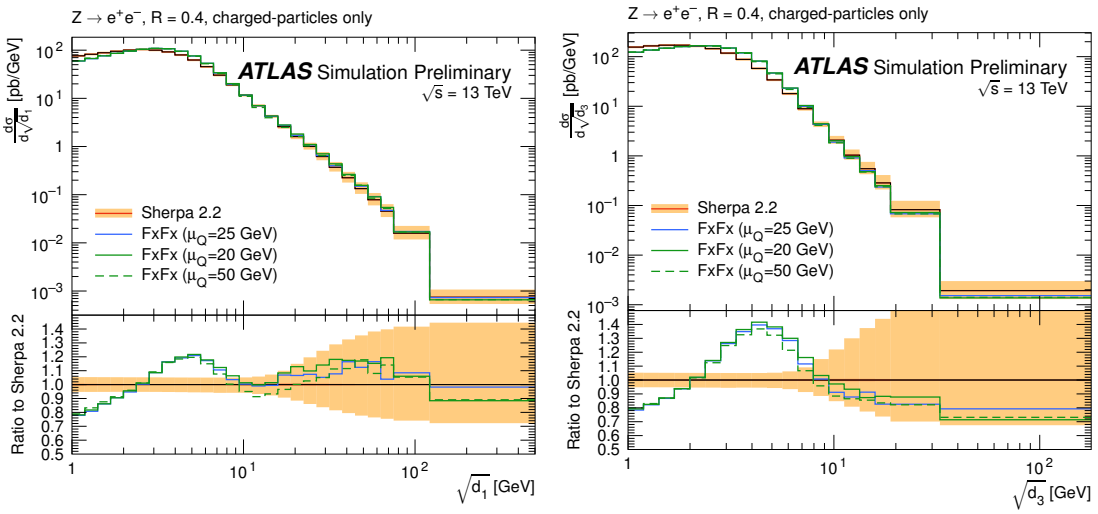

(a) (b)

Figure 2: Predictions for the differential cross sections as a function of first-order splitting scale, $\sqrt{d_1}$ (left), and of the third-order splitting scale, $\sqrt{d_3}$ (right), in the k_t algorithm using a jet-radius parameter of R = 0.4 [23] from `Sherpa 2.2` (red) and `MG5_aMC@NLO` using FxFx using μ_Q of 20 GeV (blue), 25 GeV (solid green) and 50 GeV (dashed green). These plots are taken from Ref. [2].

In Figure 3(a), the four-lepton invariant mass, which is an observable quite insensitive to higher-order QCD effects, shows good agreement above the ZZ threshold between the two generators. The deviations below this threshold can be related to differences in both the QCD and the electroweak shower which is fully based on `Pythia8` in case of `PowhegBox` while `Sherpa` uses its own shower model. Higher-order electroweak corrections have been studied and it has been found that they can also significantly affect several observables, particularly in the tails of the distributions. In Figure 3(b), a comparison of the differential cross section ($d\sigma/dp_{\mathrm{T}}^{ZZ}$) predicted by `Sherpa` and `PowhegBox` is shown. While the predictions of both generators are similarly corrected for higher-order electroweak effects, there is an additional reweighting applied for `PowhegBox` intended to bring it from NLO to approximately NNLO QCD accuracy.

Semi leptonic diboson processes As regards the generators setup, an overview is given in Table 2. Figure 4 focuses on the comparison among different generators for the invariant mass of the reconstructed hadronically decaying boson, $m(j_1, j_2)$, for all diboson processes considered. It

		$VV+0j$	$+1j$	$+2j$	$+3j$	$+\geq 4j$
$VV = WW, WZ$	`Sherpa v2.1.1`	NLO	LO	LO	LO	PS
	`Sherpa v2.2`	NLO	NLO	LO	LO	PS
	`PowhegBox+Py8/Herwig++`	NLO	LO	PS	PS	PS
$VV = ZZ$	`Sherpa v2.1.1`	NLO	NLO	LO	LO	PS
	`Sherpa v2.2`	NLO	NLO	LO	LO	PS
	`PowhegBox+Py8/Herwig++`	NLO	LO	PS	PS	PS

Table 2: Overview of process accuracies for the chosen generators.

has been found that the `PowhegBox` predictions are consistent with each other, indipendent of the

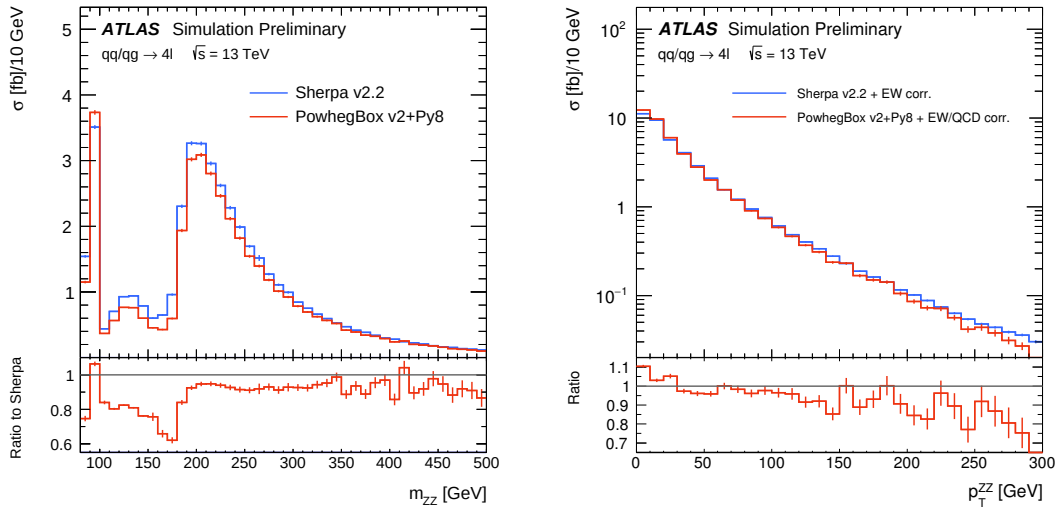

(a) (b)

Figure 3: (a) Comparison of shapes ($d\sigma/dm_{ZZ}$) normalised to the samples' cross section and combining all four channels as predicted by PowhegBox and Sherpa; (b) Differential cross section predictions ($d\sigma/dp_{TT}$) of Sherpa and PowhegBox both corrected for higher-order electroweak effects and additional incorporation of QCD effects in PowhegBox. These plots are taken from Ref. [3].

choice from the program used to implement the showering and that they are, in general, softer than the Sherpa v2.2 ones. A similar conclusion can be drawn if analysing the $WZ(\to \ell\ell)$ and the $WZ(\to \nu\nu)$ channels.

Electroweak diboson production with jets Electroweak diboson production with at least two jets includes vector boson scattering (VBS) diagrams, where the two "tagging" jets recoil against the (heavy) gauge bosons. The resulting leptonic final states include the $4\ell jj$, as well as the $2\ell 2\nu jj$ final states, where the two lepton charges can be the same or opposite sign. An overview of the accuracy achieved with the chosen generators is given in Table 3. A comparison of predicted kinematic distributions from MG5_aMC@NLO and VBFNLO, both showered with Pythia8 is shown in Figure 5: these distributions are found to be similar.

Table 3: Accuracies of the chosen generators for the listed electroweak processes.

		$VV+2j$	$VV+3j$	$VV+\geq 4j$
$VVjj = \ell^{\pm}\ell^{\mp}2\nu jj$	VBFNLO+Py8	LO	PS	PS
	MG5_aMC@NLO+Py8	LO	PS	PS
$VVjj = \ell^{\pm}\ell^{\pm}2\nu jj$	Sherpa v2.1.1	LO	PS	PS
	PowhegBox+Py8	NLO	LO	PS

Furthermore, the comparison between the leading jet p_{T} distribution predicted by PowhegBox and Sherpa can be found in Figure 6(a); PowhegBox prediction is overall in agreement within uncertainties with what is seen in Sherpa. The systematic variations for events generated with PowhegBox are derived using the PowhegBox internal reweighting scheme. The resulting

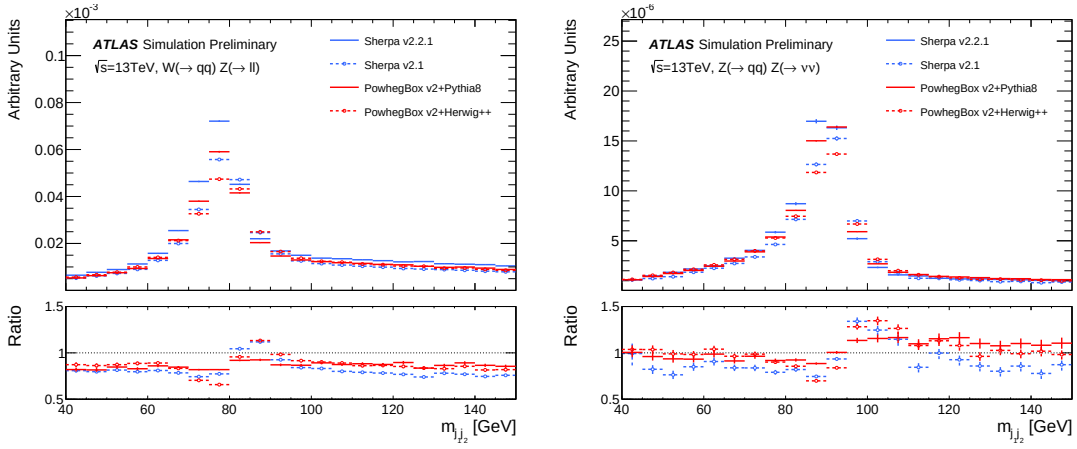

(a) (b)

Figure 4: Comparison of the invariant dijet mass $m(j_1, j_2)$ distribution in two different semileptonic final states at 13 TeV. The lower panel shows the ratio of each distribution with respect to the `Sherpa v2.2` prediction. These plots are taken from Ref. [3].

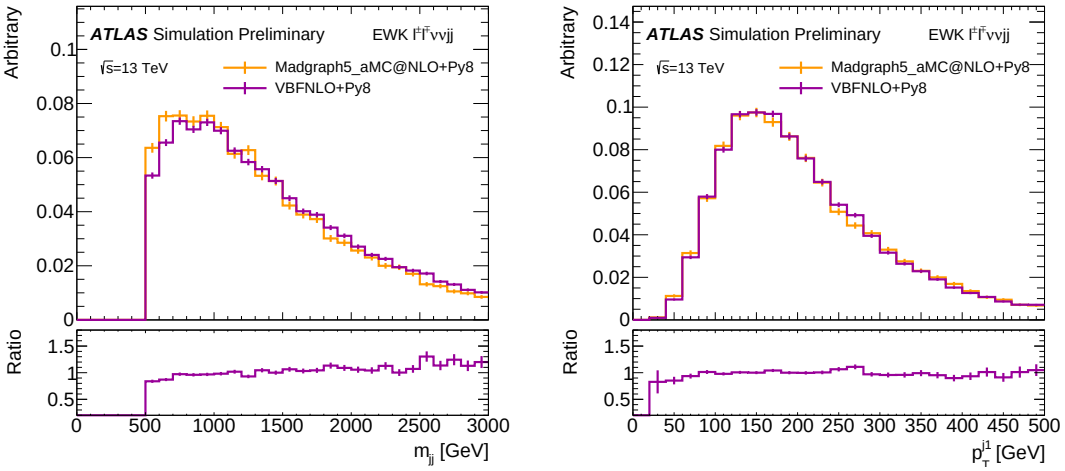

(a) (b)

Figure 5: Comparison of predicted kinematic distributions from `MG5_aMC@NLO` and `VBFNLO`, both showered with `Pythia8`, for m_{jj} (left) and leading jet p_{T} (right). These plots are taken from Ref. [3].

weights include renormalisation scale and factorisation scale. There are eight scale variations corresponding to factors of 1/2 or 2 applied independently of the renormalisation and factorisation scales, as shown in Figure 6(b) for the dijet system invariant mass distribution. The impact of scale variation is moderate (2-3%) for m_{j_1,j_2} up to 4 TeV, and then it becomes larger, rising up to 10-15% for $m_{j_1,j_2} \approx 7$ TeV.

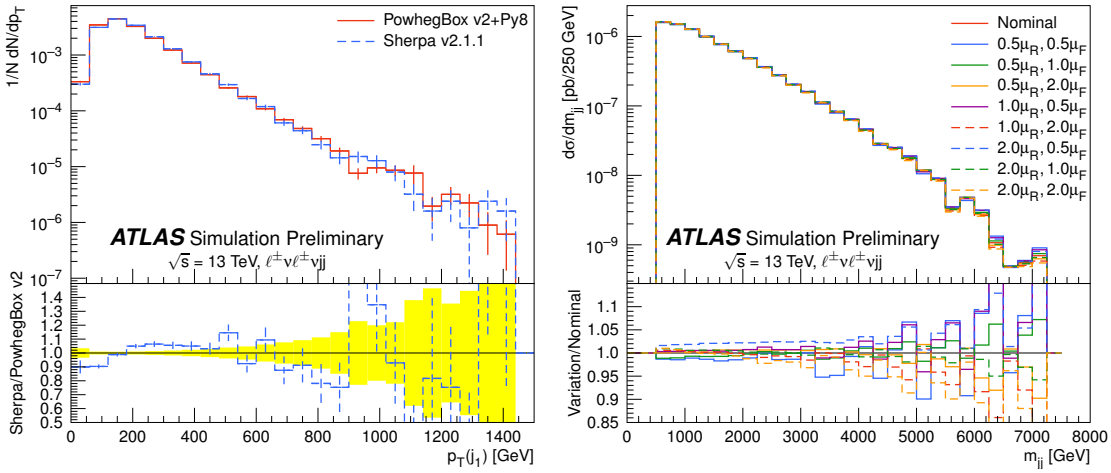

(a) (b)

Figure 6: (a) Comparison between the leading jet p_{T} distribution predicted by `PowhegBox` and `Sherpa`. The yellow band represents the statistical uncertainty of the `PowhegBox` sample; (b) Impact of scale variations on the dijet invariant mass m_{jj}. These plots are taken from Ref. [3].

References

[1] ATLAS Collaboration, *The ATLAS Experiment at the CERN Large Hadron Collider*, *JINST* **3** (2008) S08003, DOI:10.1088/1748-0221/3/08/S08003.

[2] ATLAS Collaboration, *ATLAS simulation of boson plus jets processes in Run 2*, ATL-PHYS-PUB-2017-006, 2017, URL: https://cds.cern.ch/record/2261937/.

[3] ATLAS Collaboration, *Multi-Boson Simulation for 13 TeV ATLAS Analyses*, ATL-PHYS-PUB-2017-005, 2017, URL: https://cds.cern.ch/record/2119986/.

[4] T. Gleisberg et al., *Event generation with SHERPA 1.1*, *JHEP* **02** (2009) 007, arXiv:0811.4622 [hep-ph], DOI:10.1088/1126-6708/2009/02/007.

[5] S. Schumann and F. Krauss, *A Parton shower algorithm based on Catani-Seymour dipole factorisation*, *JHEP* **03** (2008) 038, arXiv:0709.1027 [hep-ph], DOI:10.1088/1126-6708/2008/03/038.

[6] S. Höche et al., *QCD matrix elements and truncated showers*, *JHEP* **05** (2009) 053, arXiv:0903.1219 [hep-ph], DOI:10.1088/1126-6708/2009/05/053.

[7] S. Catani et al., *QCD matrix elements + parton showers*, *JHEP* **11** (2001) 063, arXiv:hep-ph/0109231, DOI:10.1088/1126-6708/2001/11/063.

[8] S. Höche et al., *QCD matrix elements + parton showers: The NLO case*, *JHEP* **04** (2013) 027, arXiv:1207.5030 [hep-ph], DOI:10.1007/JHEP04(2013)027.

[9] J. Alwall et al., *The automated computation of tree-level and next-to-leading order differential cross sections, and their matching to parton shower simulations*, *JHEP* **07** (2014) 079, arXiv:1405.0301 [hep-ph], DOI:10.1007/JHEP07(2014)079.

[10] T. Sjostrand, S. Mrenna and P. Skands, *A brief introduction to PYTHIA 8.1*, *Comput. Phys. Commun.* **178** (2008) 852, arXiv:0710.3820 [hep-ph], DOI:10.1016/j.cpc.2008.01.036.

[11] L. Lonnblad, *Correcting the color dipole cascade model with fixed order matrix elements*, *JHEP* **05** (2002) 046, arXiv:hep-ph/0112284, DOI:10.1088/1126-6708/2002/05/046.

[12] ATLAS Collaboration, *ATLAS Run 1 Pythia8 tunes*, ATL-PHYS-PUB-2014-021, 2014, URL: https://cds.cern.ch/record/1966419.

[13] R. Frederix and S. Frixione, *Merging meets matching in MC@NLO*, *JHEP* **12** (2012) 061, arXiv:1209.6215 [hep-ph], DOI:10.1007/JHEP12(2012)061.

[14] S. Alioli et al., *A general framework for implementing NLO calculations in shower Monte Carlo programs: the POWHEG BOX*, *JHEP* **06** (2010) 043, arXiv:1002.2581 [hep-ph], DOI:10.1007/JHEP06(2010)043.

[15] K. Hamilton, P. Nason and G. Zanderighi, *MINLO: Multi-Scale Improved NLO*, *JHEP* **10** (2012) 155, arXiv:1206.3572 [hep-ph], DOI:10.1007/JHEP10(2012)155.

[16] K. Hamilton et al., *Merging H/W/Z + 0 and 1 jet at NLO with no merging scale: a path to parton shower + NNLO matching*, *JHEP* **05** (2013) 082, arXiv:1212.4504 [hep-ph], DOI:10.1007/JHEP05(2013)082.

[17] ATLAS Collaboration, *Example ATLAS tunes of Pythia8, Pythia6 and Powheg to an observable sensitive to Z boson transverse momentum*, ATL-PHYS-PUB-2013-017, 2013, URL: https://cds.cern.ch/record/1629317.

[18] S. Dulat et al., *New parton distribution functions from a global analysis of quantum chromodynamics*, *Phys. Rev* **D93** (2016) 033006, arXiv:1506.07443 [hep-ph], DOI:10.1103/PhysRevD.93.033006.

[19] J. Pumplin et al., *New generation of parton distributions with uncertainties from global QCD analysis*, *JHEP* **07** (2002) 012, arXiv:0201195 [hep-ph], DOI:10.1088/1126-6708/2002/07/012.

[20] ATLAS Collaboration, *Measurements of the production cross section of a Z boson in association with jets in pp collisions at* $\sqrt{s}$ *= 13 TeV with the ATLAS detector*, *Eur. Phys. J.* **C77** (2017) 361, arXiv:1702.05725 [hep-ex].

[21] S. Catani et al., *Longitudinally invariant* k_t *clustering algorithms for hadron hadron collisions*, *Nucl. Phys.* **B406** (1993) 187-224, DOI:10.1016/0550-3213(93)90166-M.

[22] Gavin P. Salam, *Towards Jetography*, *Eur. Phys. J.* **C67** (2010) 637-686, arXiv:0906.1833 [hep-ph], DOI:10.1140/epjc/s10052-010-1314-6.

[23] ATLAS Collaboration, *Measurement of the* k_t *splitting scales in* $Z \to \ell\ell$ *events in pp collisions at* $\sqrt{s} = 8$ *TeV with the ATLAS detector*, *JHEP* **08** (2017) 026, arXiv:1704.01530 [hep-ex], DOI:10.1007/JHEP08(2017)026.